12-1-2022

Cisplatin exposure acutely disrupts mitochondrial bioenergetics in the zebrafish lateral-line organ

David S Lee

Angela Schrader

Mark Warchol

Lavinia Sheets

Hearing Research 426 (2022) 108513

Contents lists available at ScienceDirect

Hearing Research

journal homepage: www.elsevier.com/locate/heares

Cisplatin exposure acutely disrupts mitochondrial bioenergetics in the zebrafish lateral-line organ

David S. Lee[a,*], Angela Schrader[a], Mark Warchol[a,b], Lavinia Sheets[a,c]

[a] Department of Otolaryngology – Head and Neck Surgery, Washington University School of Medicine, 660 S. Euclid Ave. Campus Box 8115, St. Louis, MO 63110, USA
[b] Department of Neuroscience, Washington University School of Medicine, St. Louis, MO 63110, USA
[c] Department of Developmental Biology, Washington University School of Medicine, St. Louis, MO 63110, USA

ARTICLE INFO

Article history:
Received 1 March 2022
Revised 18 April 2022
Accepted 2 May 2022
Available online 7 May 2022

Keywords:
Cisplatin ototoxicity
Zebrafish
Mitochondrial dysfunction
Mitochondrial bioenergetics

ABSTRACT

Cisplatin is a commonly used chemotherapeutic agent that causes debilitating high-frequency hearing loss. No targeted therapies currently exist to treat cisplatin ototoxicity, partly because the underlying mechanisms of cisplatin-induced hair cell damage are not completely defined. Zebrafish may offer key insights to cisplatin ototoxicity because their lateral-line organ contains hair cells that are remarkably similar to those within the cochlea but are optically accessible, permitting observation of cisplatin injury in live intact hair cells. In this study, we used a combination of genetically encoded biosensors in zebrafish larvae and fluorescent indicators to characterize changes in mitochondrial bioenergetics in response to cisplatin. Following exposure to cisplatin, confocal imaging of live intact neuromasts demonstrated increased mitochondrial activity. Staining with fixable fluorescent dyes that accumulate in active mitochondria similarly showed hyperpolarized mitochondrial membrane potential. Zebrafish expressing a calcium indicator within their hair cells revealed elevated levels of mitochondrial calcium immediately following completion of cisplatin treatment. A fluorescent ROS indicator demonstrated that these changes in mitochondrial function were associated with increased oxidative stress. After a period of recovery, cisplatin-exposed zebrafish demonstrated caspase-3-mediated apoptosis. Altogether, these findings suggest that cisplatin acutely disrupts mitochondrial bioenergetics and may play a key role in initiating cisplatin ototoxicity.

1. Introduction

Cisplatin is a chemotherapeutic agent that is commonly used in the treatment of solid tumors. Cisplatin's anti-tumor activities arise from its ability to intercalate into DNA, thereby promoting the formation of DNA adducts that block transcription and trigger apoptosis in rapidly dividing cells (Ciccarelli et al., 1985; Ormerod et al., 1994; Pinto and Lippard, 1985). However, treatment with cisplatin also causes permanent hearing loss in more than 50% of adults (Brock et al., 2012; Schmitt and Page, 2018) and up to 60% of children (Brock et al., 2012; Knight et al., 2017). Hair cells are not mitotically active, but they are still susceptible to cisplatin injury, suggesting that cross-linking of nuclear DNA may not be the predominant mechanism of cisplatin-induced hearing loss. Numerous studies have suggested that the pathologic generation of reactive oxygen species (ROS) plays a critical role in cisplatin ototoxicity (Sheth et al., 2017). However, multiple pathways can mediate oxidative stress, and it is unclear how cisplatin drives ROS production (Gentilin et al., 2019; Kros and Steyger, 2019; Sheth et al., 2017).

Mitochondria are one of the main sources of endogenous ROS, and they have been strongly implicated to play a role in cisplatin ototoxicity. *In vitro* studies of cancer and non-cancer cell lines demonstrate that cisplatin exposure generates mitochondrial-dependent oxidative stress, and that more metabolically active cells show greater susceptibility to cisplatin (Marullo et al., 2013). Mitochondria are also involved in the later phases of cisplatin-induced hair cell death. In Mongolian gerbils, cisplatin ototoxicity was associated with increased expression of Bax, a protein that induces the mitochondrial apoptotic pathway, and decreased levels of Bcl-2, a protein that promotes cell survival, throughout all turns of the cochlea (Alam et al., 2000). Similar findings were recapit-

* Corresponding author at: Department of Otolaryngology – Head and Neck Surgery, Washington University School of Medicine, 660 S. Euclid Ave. Campus Box 8115, St. Louis, MO 63110, USA.
E-mail address: david.s.lee@wustl.edu (D.S. Lee).

https://doi.org/10.1016/j.heares.2022.108513

ulated in cisplatin-treated guinea pigs (Wang et al., 2004) and in UB/OC-1 cells (Borse et al., 2017), suggesting that impaired mitochondrial function is a significant contributor to cisplatin ototoxicity. However, the specific cellular events that drive mitochondrial dysfunction, oxidative stress, and hair cell death remain an open question.

A major barrier to understanding the cellular mechanisms that underlie cisplatin-induced hair cell death is an inability to observe dynamic processes within the cochlea. Research on cochlear cisplatin ototoxicity has been complemented by studies using zebrafish models because they possess hair cells along the surface of their body within the lateral-line sensory system in organs called neuromasts (Domarecka et al., 2020; Wertman et al., 2020). The superficial location of neuromasts enables reliable drug treatment protocols and optical accessibility for live-imaging techniques to directly observe hair cell response to cisplatin *in vivo*.

The goal of the present study was to investigate the effect of cisplatin on hair cell mitochondrial activity and homeostasis within intact neuromasts of the zebrafish lateral-line organ. Transgenic zebrafish with genetically encoded biosensors were treated with cisplatin for two hours and their neuromasts were imaged live immediately after completion of drug exposure. Hair cell mitochondrial activity (as measured by uptake of tetramethylrhodamine ethyl ester; TMRE) and hair cell mitochondrial calcium levels (as measured by the genetically encoded indicator mitoGCaMP3 fluorescence) were both increased in response to cisplatin treatment. These changes in mitochondrial function were also associated with an increase in ROS production. Subsequent canonical activation of caspase-3-mediated apoptosis in hair cells treated with cisplatin was observed, suggesting that mitochondrial dysfunction may be an essential component of cisplatin ototoxicity. Cumulatively, these results indicate that changes in hair cell mitochondrial function may be among the first events to occur following cisplatin exposure and suggest that the intrinsic (mitochondrial) apoptosis pathway drives cisplatin-induced hair cell death.

2. Material and methods

2.1. Zebrafish husbandry and lines

All experiments and procedures on zebrafish were performed in accordance with the Washington University Institutional Animal Use and Care Committee.

Adult zebrafish were maintained in group housing and standard conditions at the Washington University Zebrafish Facility. Embryos were maintained in embryo media (EM: 15 mM NaCl, 0.5 mM KCl, 1 mM $CaCl_2$, 1 mM $MgSO_4$, 0.15 mM KH_2PO_4, 0.042 mM Na_2HPO_4, 0.714 mM $NaHCO_3$) at 28 °C with a 14-hour light and 10-hour dark cycle (Westerfield, 2000). After 4 days post-fertilization (dpf), larvae were raised in 100 – 200 mL EM in 250-mL plastic beakers and fed rotifers daily. The sex of the animal was not considered because it cannot be determined in zebrafish larvae. Experiments were started in the mid-morning and completed by the late afternoon. At their conclusion, zebrafish were euthanized by quick chilling to 4 °C in an ice water bath.

The transgenic lines *Tg(myo6b:mitoGCaMP3)* (allele number: w119Tg) and *Tg(TNKS1bp1:EGFP)* (allele number: y229Gt) were used in this study (Behra et al., 2012; Esterberg et al., 2014). *Tg(myo6b:mitoGCaMP3)* fish were used to quantify mitochondrial calcium levels in response to cisplatin. *Tg(TNKS1bp1:EGFP)* fish label neuromast supporting cells and were used to outline neuromast hair cells in live imaging experiments. This approach was used instead of labeling hair cells with 4′,6-Diamidino-2-Phenylindole (DAPI) in live imaging experiments because imaging DAPI-labeled nuclei requires a high-frequency laser, which may unintentionally injure hair cells during live acquisition. Larval zebrafish were screened for transgenic fluorophores at 3 – 5 dpf under sedation with 0.01% tricaine in EM using a Leica MZ10 F stereomicroscope with fluorescence equipped with a GFP and a DSR filter set.

2.2. Exposure of neuromast hair cells to cisplatin

Lateral-line hair cells were treated with cisplatin, a chemotherapeutic drug with well-established ototoxic effects (Domarecka et al., 2020; Ou et al., 2007), by exposing free-swimming zebrafish larvae at 6 dpf. Groups of ~20 – 30 larvae were placed in 25 mm cell strainers (Corning Cell Strainer) and incubated for 2 h in 30 mL of EM containing 0.1% dimethyl sulfoxide (DMSO) with either 250 μM or 1 mM cisplatin (Abcam) at 28 °C. A systematic review of cisplatin ototoxicity studies in zebrafish indicated that studies used a wide range of exposure duration (45 min to 24 h) and concentrations of cisplatin (50 uM to 1 mM). Based on these data, a relatively shorter exposure time of 2 h and moderate to high concentrations of cisplatin were used to produce a consistent hair cell lesion while minimizing systemic toxicity, emulating a clinically relevant exposure protocol.

Larvae were then rinsed 3x in 30 mL EM and incubated in various fluorescent indicators for live imaging, or were maintained in 30 mL EM for an additional 2 to 4 h, depending on the specific experiment. Control larvae underwent an identical protocol, but were treated with 0.1% DMSO. Although DMSO increases cisplatin potency and is not a required carrier for intracellular uptake, zebrafish are commonly used as a model for otoprotective drugs so experiments were designed to be generalizable to otoprotective drug studies (Domarecka et al., 2020; Uribe et al., 2013).

2.3. Live hair cell labeling, imaging, and analysis

For live imaging experiments, larvae that had just completed the treatment protocols described in Section 2.2 were incubated for 30 min in either 8 mL of 250 nM TMRE (Invitrogen) in EM or 1 mL of 5 or 10 μM CellROX Deep Red (Invitrogen) in darkness and then rinsed 2x in EM. TMRE and CellROX Deep Red were used to measure mitochondrial activity and oxidative stress, respectively. Two different concentrations of CellROX Deep Red were used to account for batch-to-batch variability in the fluorescent indicator.

Larvae (6 dpf) underwent live imaging, following previously published methods (Holmgren et al., 2021). Briefly, individual larvae were sedated with 30 mL EM with 0.01% tricaine and mounted lateral-side up within a small amount of 2% low-melt agarose on a FluoroDish (World Precision Instruments, Cat# FD3510). Mounted larvae were then submerged in ~0.5 – 1 mL EM with 0.01% tricaine. Z-stack images (step size of 1 μm) from neuromasts L3 – L6 of the posterior lateral-line were acquired with an ORCA-Flash 4.0 V3 camera (Hamamatsu) using a Leica DM6 Fixed Stage microscope with an X-Light V2TP spinning disk confocal (60 μm pinholes) and a 63x/0.9 N.A. water immersion objective. TMRE imaging used a 555 nm wavelength laser (RFP), operating at 20% power, with 120 ms/frame exposure time. CellROX Deep Red imaging used a 646 nm wavelength laser (Cy5), operating at 20% power, with 150 ms/frame exposure time. Images of mitoGCaMP3 activity were obtained using a 470 nm wavelength laser (GFP), at 20% power and 120 ms/frame acquisition times. TNKS1bp1:EGFP fish were imaged with a 470 nm wavelength laser (GFP), at 20% power and 150 ms/frame scan time. All image acquisition was controlled by MetaMorph software (Molecular Devices).

Digital images of neuromasts were processed using ImageJ software (Schneider et al., 2012) and Adobe Illustrator. Single-channel z-stacks were individually measured for each neuromast (L3 – L6). Background subtraction was performed using a rolling ball radius at the following sizes: 100 pixels for TMRE, and 150 pixels for

mitoGCaMP3 and CellROX Deep Red. Maximum intensity projections of each z-stack were generated, their corresponding neuromast was outlined, and mean fluorescent pixel intensities of each neuromast were measured. Lastly, to account for fish-to-fish variability, the mean fluorescent intensities of neuromasts originating from the same zebrafish were averaged. Within each experimental trial, the average intensity per zebrafish was normalized to the median value of the average intensity per control zebrafish to address experiment-to-experiment variability.

2.4. Whole-mount immunohistochemistry, imaging, and analysis of fixed specimens

2.4.1. MitoTracker experiments

For fixable MitoTracker experiments, neuromast hair cell labeling was performed as previously described (Holmgren and Sheets, 2021). MitoTracker was used as an additional indicator of mitochondrial activity. Briefly, larvae that had just completed 2 hr of cisplatin exposure were incubated for 4 min in 15 mL EM with 5 μg/mL 4′,6-Diamidino-2-Phenylindole (DAPI; Invitrogen) at 28 °C in the dark, and then rinsed 2x in 30 mL EM. Larvae were then incubated for 30 min in 15 mL EM containing 500 nM MitoTracker Red CMXRos and 500 nM MitoTracker Deep Red at 28 °C in darkness, followed by 3x rinses in 30 mL EM. At this point, specimens were euthanized by rapid cooling of fish medium, and fixed overnight in 4% paraformaldehyde in 0.1 M phosphate-buffered solution (PBS pH = 7.4) at 4 °C. The following day, fixed specimens were rinsed 3x in PBS. MitoTracker-treated larvae were then mounted on glass slides in elvanol (13% w/v polyvinyl alcohol, 33% w/v glycerol, 1% w/v DABCO (1,4 diazobicylo[2,2,2] octane) in 0.2 M Tris, pH 8.5) and covered with #1.5 cover slips prior to imaging.

Larvae stained with MitoTracker dyes were imaged on an X-Light V2TP spinning disk confocal microscope, using a 63x/0.9 N.A. oil immersion objective (Leica). Image stacks of posterior lateral-line neuromasts L4 – L6 were acquired, at 1 μm step size. MitoTracker CMXRos Z-acquisition parameters were 555 nm wavelength laser (RFP) set to 20% power and 120 ms/frame. MitoTracker Deep Red data were collected with a 646 nm wavelength laser (Cy5), at 20% power and100 ms/frame. DAPI images were acquired with a 405 nm wavelength laser, at 20% power and 100 ms/per frame. All image acquisition was controlled by MetaMorph software (Molecular Devices).

Digital images were processed using ImageJ software (Schneider et al., 2012) and Adobe Illustrator. Whole neuromast fluorescence intensity was measured as in Section 2.3 with a rolling ball radius of 200 pixels for both MitoTracker dyes. The mean intensity of the fluorescent indicators for each neuromast was measured. Average neuromast intensity was normalized to the median value of the average neuromast intensity observed in DMSO controls.

2.4.2. Caspase-3 experiments

After completing a 2 h exposure to cisplatin followed by a 2 h recovery period in EM, fish were euthanized by rapid chilling and fixed in paraformaldehyde as described in Section 2.4.1. In preparation for cleaved caspase-3 labeling, fixed specimens were blocked for 2 h with 5% normal horse serum (NHS) in PBS with 1% Triton X-100, at room temperature and with gentle agitation. The blocking solution was then replaced with primary antibodies diluted in PBS, 2% NHS, and 1% Triton X-100, and incubated overnight at room temperature and with gentle agitation. The primary antibodies were HCS-1 (hair cells, mouse monoclonal, 1:500, DSHB, University of Iowa), and anti-cleaved caspase-3 (rabbit polyclonal, 1:400, Cell Signaling). The following day, larval zebrafish were rinsed 3x in PBS, incubated for 2 h in DAPI (5 μg/mL) and secondary antibodies (anti-mouse IgG, conjugated to Alexa Fluor 488 and anti-rabbit IgG, conjugated to Alexa Fluor 555; Invitrogen), both diluted 1:500 in PBS with 2% NHS and 1% Triton X-100, at room temperature in darkness. Specimens were then rinsed 3x in PBS and mounted as described above.

The posterior lateral-line neuromasts (L3 – L6) of fixed zebrafish immunolabeled with HCS-1 and anti-cleaved caspase-3 were imaged with an LSM 700 laser scanning confocal microscope (Carl Zeiss). Each neuromast was evaluated for the presence or absence of cleaved caspase-3 labeling in hair cells and data were expressed as the percentage of neuromasts with activated caspase-3. Z-stack images of representative cisplatin-exposed and control neuromasts (step size of 0.29 μm) were acquired on the scanning confocal microscope using a 63×1.4 N.A. Plan-Apochromat oil immersion objective (Carl Zeiss).

2.5. Statistical analysis

Statistical analyses were performed with Prism 9 (GraphPad Software Inc). Normality of data were determined with the D'Agostino-Pearson test. Statistical significance between two groups was determined using an unpaired Student's *t*-test or a Mann-Whitney *U* test, as appropriate. Comparison of multiple groups was evaluated by one-way ANOVA or Kruskal-Wallis test with appropriate *post hoc* tests as needed.

3. Results

3.1. Cisplatin exposure causes an acute increase in mitochondrial activity in hair cells

Although hair cells are susceptible to cisplatin injury, they do not proliferate, suggesting that cisplatin-induced hearing loss takes place through a mechanism other than the induction of adducts in nuclear DNA (Martens-de Kemp et al., 2013; Ou et al., 2007; Yimit et al., 2019). Since hair cells are highly metabolically active and cisplatin may accumulate within hair cell mitochondria (Yang et al., 2006), one hypothesis is that cisplatin directly affects mitochondrial bioenergetics, leading to mitochondrial dysfunction and subsequent oxidative stress. Initial experiments characterized the association between mitochondrial activity and cisplatin exposure. Prior *in vivo* and *in vitro* studies demonstrate increased mitochondrial ROS and upregulated proteins associated with mitochondrial-induced apoptosis after cisplatin exposure (Alam et al., 2000; Borse et al., 2017; Wang et al., 2004). To explore acute changes in hair cell mitochondrial activity following cisplatin treatment, live intact neuromasts were imaged after uptake of TMRE, a cell-permeant fluorescent indicator sequestered by active mitochondria. Confocal imaging of *Tg(TNKS1bp1:EGFP)* zebrafish at 6 dpf captured mitochondrial activity immediately following a 2 h exposure to 250 μM cisplatin or to 0.1% DMSO (control) (Fig. 1A – F). Each fish was considered as a single biological sample. Data were derived from confocal images of neuromasts L3 – L6 (4 neuromasts/zebrafish, $n = 15 – 16$ zebrafish/group, $N = 4$ experimental trials), and indicate an acute increase in hair cell TMRE intensity in cisplatin-treated zebrafish (Fig. 1G, $^{**}p = 0.0021$, unpaired t-test).

We next compared changes in mitochondrial membrane potential in response to two different doses of cisplatin. Fish (6 dpf) were loaded with CMXRos and MitoTracker Deep Red, which are fixable fluorescent indicators of mitochondrial membrane potential in live cells. Following dye loading, fish were treated for 2 h with 0.1% DMSO (control), 250 μM cisplatin, or 1 mM cisplatin. They were then rinsed in EM, stained with DAPI and MitoTracker, euthanized, and fixed. Confocal images of neuromasts L4 – L6 were obtained, to determine the effect of cisplatin on mitochondrial membrane potential (Fig. 2A – I; 3 neuromasts/zebrafish, $n = 45$ neuromasts/group, $N = 3$ experimental trials). Data derived from these

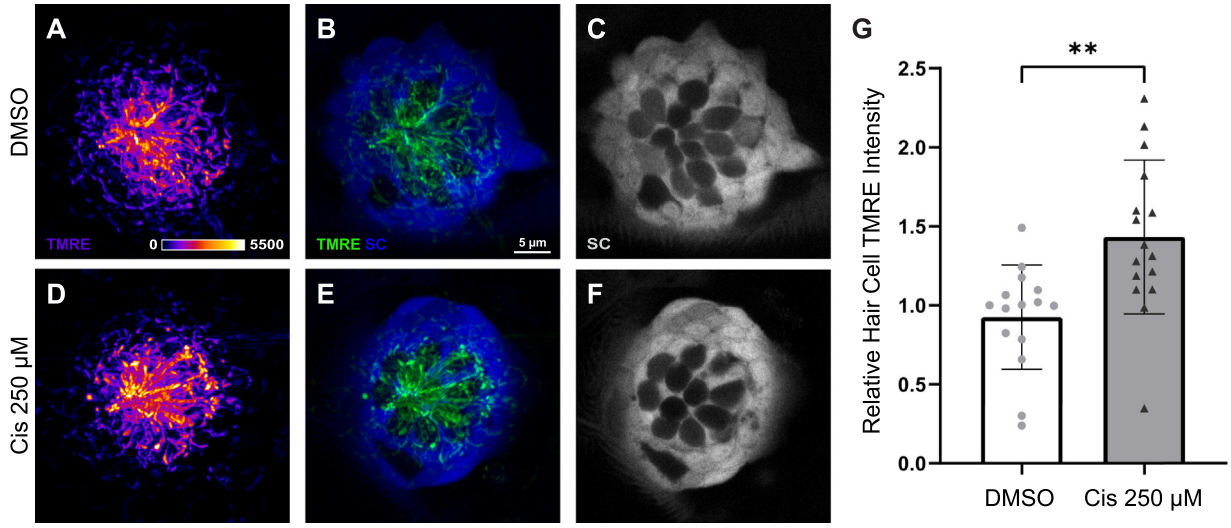

Fig. 1. Hair cell mitochondrial activity increases following cisplatin exposure. Maximum-intensity projections of confocal images show TMRE-loaded *Tg(TNKS1bp1:EGFP)* zebrafish neuromasts with GFP-expressing supporting cells (SC) and GFP-negative hair cells after 2 h treatment with 0.1% DMSO (A-C) and 250 µM cisplatin (D – F). TMRE labeling is observed most prominently in hair cells (A-B; D-E). Mean hair cell TMRE intensity (normalized to control) was elevated in the cisplatin-exposed neuromasts (G, $^{**}p = 0.0021$, unpaired t-test). $n = 15$ – 16 zebrafish. $N = 4$ experimental trials. Error bars = standard deviation.

images demonstrated that mitochondrial membrane hyperpolarization trended upwards in response to increasing concentrations of cisplatin (Fig. 2J – K). However, Tukey's multiple comparisons test of MitoTracker CMXRos only detected a significant difference between DMSO and 1 mM cisplatin (Fig. 2J, $^{**}p = 0.0039$). In contrast, Tukey's multiple comparisons test of MitoTracker Deep Red showed significant differences between all three treatment conditions (Fig. 2K, $^{**}p = 0.0011$; $^{****}p < 0.0001$). Interestingly, hair cells within the same neuromast appeared to heterogeneously accumulate MitoTracker regardless of treatment group instead of being equally distributed throughout the entire neuromast. This heterogeneous uptake may indicate that there are underlying factors that affect individual hair cell susceptibility to cisplatin. When considered with the data from the TMRE experiments (Fig. 1), these observations suggest that mitochondrial activity increases following cisplatin treatment in a dose-dependent manner.

3.2. Cisplatin exposure causes acute increases in hair cell mitochondrial calcium levels and ROS production

Mitochondria serve as buffers, sensors, and modulators of intracellular calcium signaling (Rizzuto et al., 2012). Prior *in vitro* studies on cancer cells and hair cell-like cell lines demonstrate that dysregulated mitochondrial calcium handling in response to cisplatin may initiate toxic levels of ROS production and mitochondria-mediated apoptosis (Bernardi, 1999; Kleih et al., 2019; Lu et al., 2019; Zhao et al., 2022). To investigate the effect of cisplatin on mitochondrial calcium and oxidative stress, we employed confocal imaging of live intact neuromast hair cells expressing the mitochondrial calcium indicator mitoGCaMP3. *Tg(myo6b:mitoGCaMP3)* zebrafish at 6 dpf were treated for 2 h with 0.1% DMSO or 250 µM cisplatin, rinsed in EM, incubated in fluorescent ROS indicator, CellROX Deep Red, and used for live imaging. Representative images of neuromasts in the control and cisplatin groups are depicted in Fig. 3A – F. Data were derived from confocal images of neuromasts L3 – L6, demonstrating that cisplatin exposure increases hair cell mitochondrial calcium levels (Fig. 3G, $^{**}p = 0.0074$, Mann-Whitney U test, 4 neuromasts/zebrafish, $n = 32$ – 34 zebrafish/group, $N = 8$ experimental trials) and ROS production (Fig. 3H, $^{*}p = 0.014$, Mann-Whitney U test, 4 neuromasts/zebrafish, $n = 26$ – 27 zebrafish/group, $N = 7$ experimental trials). As with the mitochondrial membrane potential assays, mitochondrial calcium levels of individual hair cells within the same neuromast were heterogeneous regardless of treatment group. However, the present methods were unable to delineate whether this heterogeneity affects susceptibility to cisplatin.

3.3. Cisplatin-induced hair cell death is mediated by activated caspase-3

Prior studies indicate that cisplatin causes hair cell apoptosis by elevating the ratio of Bax to Bcl-2, resulting in mitochondrial membrane permeability, leakage of cytochrome-c and activation of canonical caspase-3-mediated apoptosis (Borse et al., 2017; Devarajan et al., 2002; Wang et al., 2004). To investigate the effect of cisplatin on mitochondrially-mediated apoptosis in neuromast hair cells, 6 dpf zebrafish were treated for 2 h with 0.1% DMSO, 250 µM cisplatin, or 1 mM cisplatin. They were then thoroughly rinsed and maintained for an additional 2 h in EM, at which point they were euthanized, fixed and processed for visualization of hair cells and cleaved caspase-3. Representative confocal images of neuromasts L3 – L6 (4 neuromasts/fish, $n = 30$ neuromasts/group, $N = 3$ experimental trials) are depicted in Fig. 4A – C, and demonstrate the presence of activated caspase-3 in hair cells of cisplatin-exposed zebrafish, but not in DMSO-exposed controls (Fig. 4D, $p < 0.0001$, Kruskal-Wallis test). Analysis of the percentage of neuromasts containing a subset of hair cells that were immunoreactive for cleaved caspase-3 suggest that cisplatin induces neuromast hair cell apoptosis at moderate (250 µM) and high (1 mM) doses (Fig. 4D, $^{**}p = 0.003$, $^{****}p < 0.0001$, Dunn's multiple comparisons test).

4. Discussion

Cisplatin is commonly used in the treatment of solid tumors in both adult and pediatric populations. Permanent hearing loss is a frequent consequence of cisplatin chemotherapy and no FDA-approved methods exist to mitigate cisplatin ototoxicity. Although mitochondria have been identified as potential drivers of cisplatin injury in hair cells (Sheth et al., 2017), characterizing changes in mitochondrial function in response to cisplatin will identify critical cellular events that result in apoptosis. While drug delivery

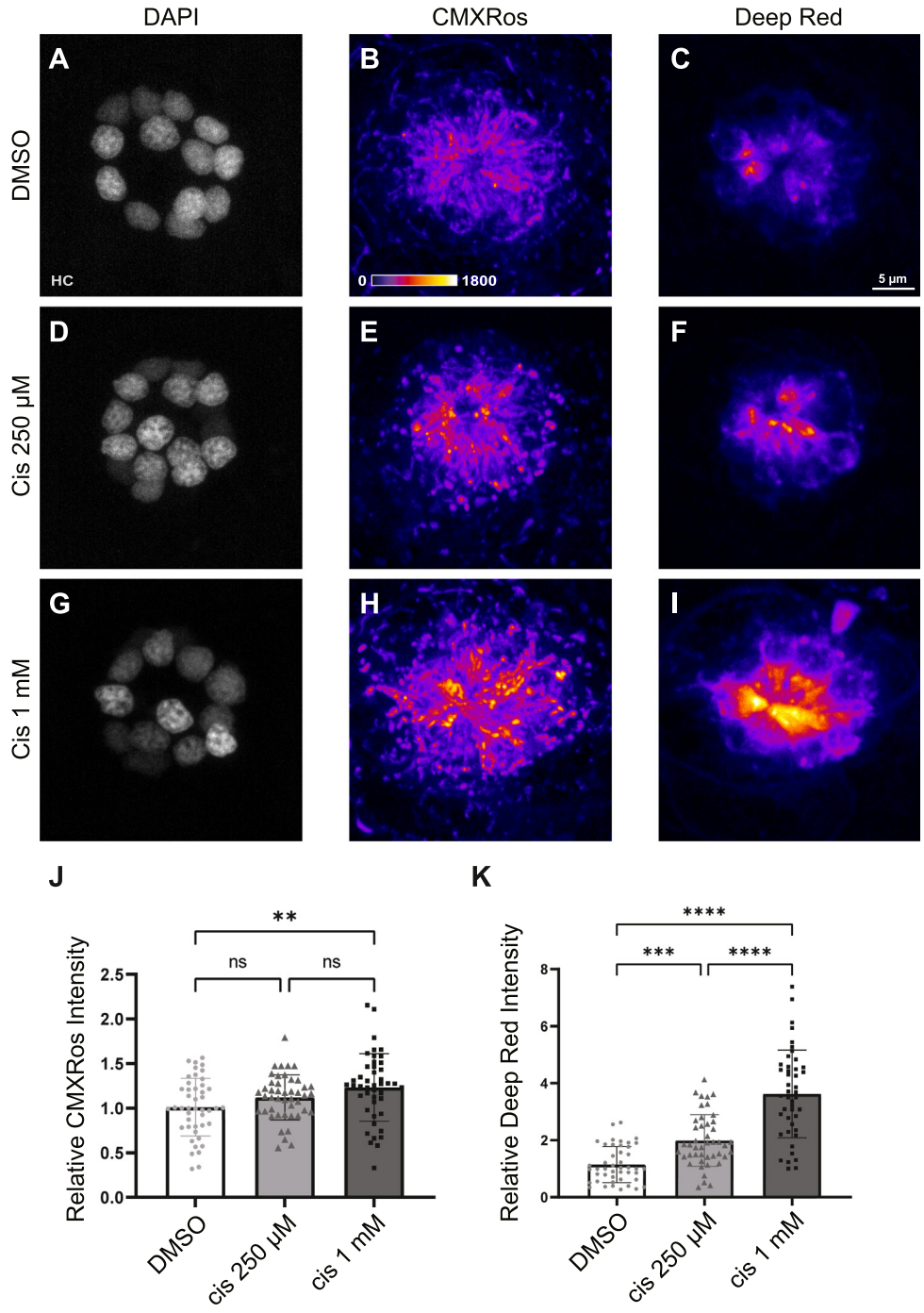

Fig. 2. The degree of cisplatin-induced mitochondrial hyperpolarization is dose dependent. Maximum-intensity projections of confocal images show neuromasts treated with 0.1% DMSO (A – C), 250 µM cisplatin (D – F), and 1 mM cisplatin (G – I). Hair cells were labeled with DAPI and mitochondria were stained with Mitotracker CMXRos and MitoTracker Deep Red. Mean intensities (normalized to control) increased in a dose-dependent manner across both MitoTracker CMXRos (J, $p = 0.0058$, one-way ANOVA) and MitoTracker Deep Red (K, $p < 0.0001$, one-way ANOVA) indicators. Post-hoc analysis with Tukey's multiple comparisons test failed to detect significant changes in mean CMXRos intensities between DMSO and 250 µM cisplatin (J, ns = 0.23) and 250 µM cisplatin and 1 mM cisplatin (J, ns = 0.24). For MitoTracker Deep Red, significant differences were observed using Tukey's multiple comparisons test between all treatment groups (K, $^{**}p = 0.0011$, $^{****}p < 0.0001$). $n = 135$ neuromasts. $N = 3$ experimental trials. Error bars = standard deviation.

to the inner ear, off-target effects, and appropriate patient selection continue to challenge successful translation of an otoprotective drug (Freyer et al., 2020; Hazlitt et al., 2018; Yu et al., 2020), understanding the effect of cisplatin on mitochondria will address a major gap in knowledge that in part, prevents the development of otoprotective therapies.

The primary functions of mitochondria are to produce ATP and mediate intracellular calcium homeostasis (Marullo et al., 2013; Rizzuto et al., 2012). Prior *in vitro* and *in vivo* studies indicate that cisplatin rapidly enters hair cells (Thomas et al., 2013), accumulates within mitochondria (Yang et al., 2006), and leads to canonical caspase-3-mediated apoptosis (Borse et al., 2017; Devarajan et al., 2002; Wang et al., 2004). While these studies have established an important framework for determining the contribution of mitochondrial dysfunction to cisplatin ototoxicity, a common limitation is that they observe the downstream effects of mitochondrial

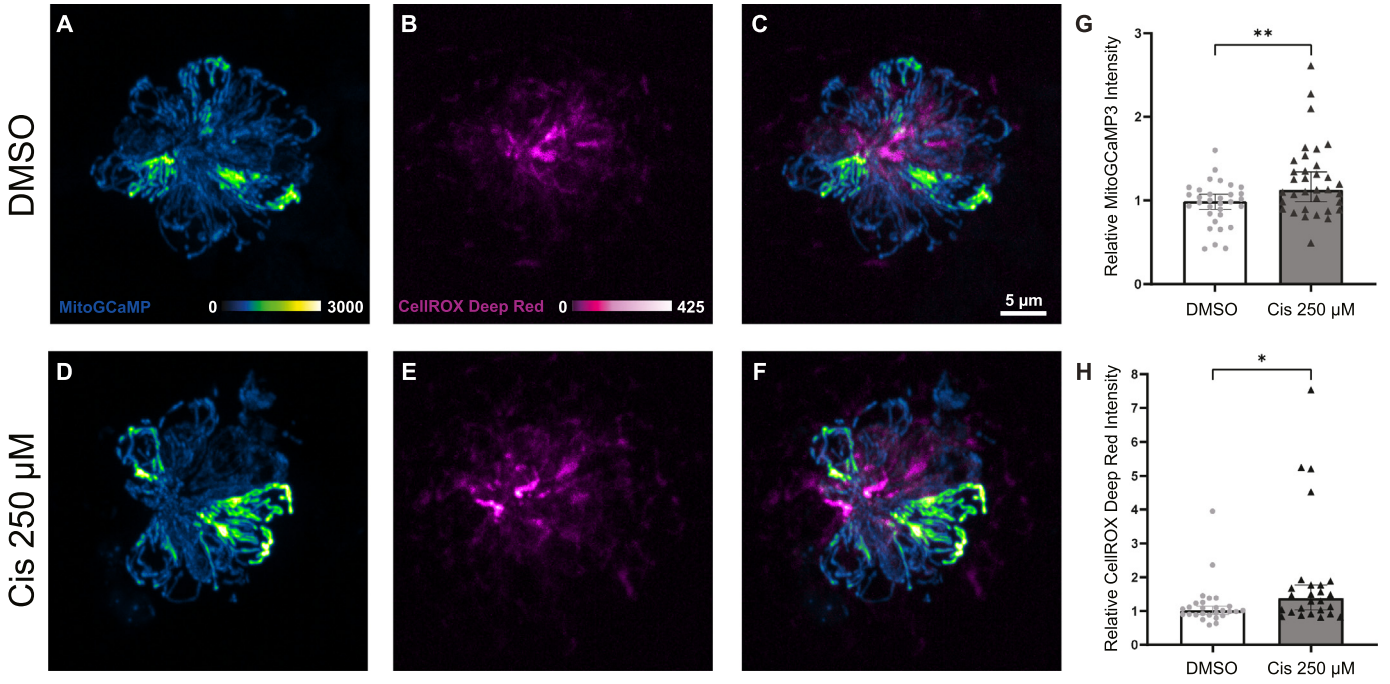

Fig. 3. Cisplatin exposure causes acute increases in mitochondrial calcium levels and ROS production. Maximum-intensity projections of confocal images show mitoGCaMP3 and CellROX Deep Red fluorescence within neuromasts of *Tg(myo6b:mitoGCaMP3)* zebrafish treated with DMSO (A – C) and 250 µM cisplatin (D – F). Zebrafish treated with cisplatin demonstrate elevated levels of relative mitoGCaMP3 intensity (G, $^{**}p = 0.0074$, Mann-Whitney U test, $n = 32$ – 34 zebrafish, $N = 8$ experimental trials) and increased CellROX Deep Red intensity (H, $^{*}p = 0.014$, Mann-Whitney U test, $n = 26$ – 27 zebrafish, $N = 7$ experimental trials). Error bars = 95% CI.

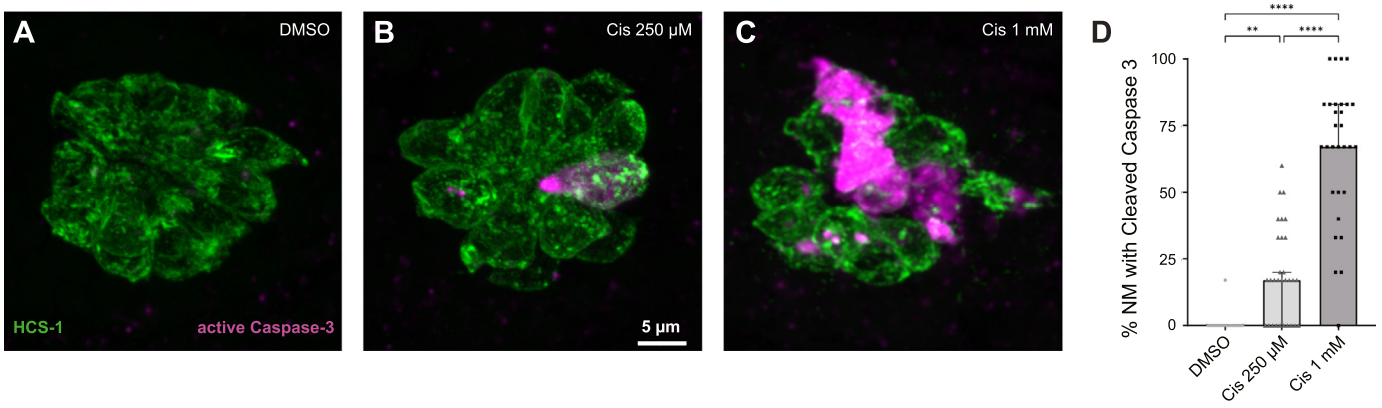

Fig. 4. Cisplatin activates caspase-3-mediated hair cell death. Maximum-intensity projections of confocal images showing HCS-1 staining of hair cell membranes and cleaved caspase-3 staining within the neuromast of 6 dpf larvae treated with 0.1% DMSO (A), 250 µM cisplatin (B), and 1 mM cisplatin (C) for 2 h, followed by recovery for 2 h. Median percentages of neuromasts with activated caspase-3 staining are greater in cisplatin-treated zebrafish compared to DMSO-treated zebrafish in a dose-dependent manner (D, $^{**}p = 0.003$, $^{****}p < 0.0001$, Dunn's multiple comparisons test). $n = 90$ neuromasts. $N = 3$ experimental trials. Error bars = 95% CI.

dysfunction and are unable to characterize dynamic changes in mitochondrial bioenergetics that occur within a live intact hair cell. In this study, we measured the intensity of fluorescent indicators and genetically encoded biosensors within live and fixed transgenic zebrafish exposed to cisplatin, in order to identify acute changes in hair cell mitochondrial function. We found that cisplatin hyperpolarized hair cell mitochondria (Figs. 1 and 2), elevated hair cell mitochondrial calcium levels (Fig. 3), and increased oxidative stress (Fig. 3) within hair cells of the zebrafish lateral line. Such knowledge enhances our understanding of when mitochondrial dysfunction begins, and further supports the notion that mitochondrial dysfunction is an essential component of cisplatin ototoxicity.

The timing of mitochondrial dysfunction after exposure to cisplatin and its association with hair cell death has not been previously characterized. A recent series of studies exploring neomycin ototoxicity have demonstrated that mitochondrial dysfunction is among the first events to occur after exposure to neomycin, beginning with excessive mitochondrial calcium uptake and hyperpolarization, followed by rapid collapse of mitochondrial membrane potential within 30 min (Esterberg et al., 2014, 2016; Owens et al., 2007). These events ultimately cause the generation of pathologic levels of ROS and subsequent hair cell death (Esterberg et al., 2016). Our data suggest that cisplatin may produce acute changes in mitochondrial bioenergetics, similar to those observed after exposure to neomycin, *e.g.*, mitochondrial hyperpolarization (Fig. 2), elevated mitochondrial calcium levels (Fig. 3), and increased hair cell ROS production (Fig. 3). These findings are consistent with studies of the mammalian ear that indicate cisplatin exposure leads to calcium accumulation in the cytosol and mitochondria of hair cells (Lu et al., 2019; Zhao et al., 2022). Since disrupted

mitochondrial bioenergetics have previously been associated with mitochondrial ROS production (Gentilin et al., 2019; Kros and Steyger, 2019; Sheth et al., 2017) and caspase-3-mediated hair cell death (Fig. 4), we propose that hyperpolarized membrane potential and elevated calcium levels immediately following cisplatin exposure may be initiating events in cisplatin ototoxicity.

Our data further indicate that there appears to be heterogenous mitochondrial activity and mitochondrial calcium levels of hair cells within the same neuromast regardless of treatment group (Figs. 2A – I, 3A and D). The biological and clinical significance of this heterogeneity remains an open question. Nonetheless, we speculate that it may represent as-yet unidentified factors that contribute to variability in hair cell vulnerability, and that these differences may be rooted in mitochondrial function. Prior studies of aminoglycoside ototoxicity report that hair cell vulnerability may be linked to cumulative mitochondrial activity, rather than acute changes in mitochondrial activity (Pickett and Raible, 2019; Pickett et al., 2018). This notion corresponds with clinical observations that age is an independent risk factor for cisplatin ototoxicity (Fernandez et al., 2019; Theunissen et al., 2015), and that the more metabolically active high-frequency outer hair cells are at greater risk of cisplatin injury than low-frequency inner hair cells (Prayuenyong et al., 2021). A limitation of this study is that the live imaging techniques used enable whole neuromast analysis at a single point in time. Such techniques cannot explore the effect of baseline mitochondrial bioenergetics on hair cell survival, which require repeated measures of individual hair cells across multiple time points. In future studies, similar methods as those used to investigate susceptibility of individual hair cells to aminoglycoside ototoxicity can be used to test the contribution of hair cell mitochondrial age, activity, and redox history on cisplatin vulnerability (Lukasz et al., 2022; Pickett et al., 2018).

The relationship between cisplatin and oxidative stress has been well established (Gentilin et al., 2019; Kros and Steyger, 2019; Sheth et al., 2017), and prior studies demonstrate that mitochondria play a key role in cisplatin-induced oxidative stress in cancer and non-cancer cell lines (Marullo et al., 2013) as well as hair cells (Li et al., 2021; Lu et al., 2022). Here, we build on this literature and demonstrate that oxidative stress occurs shortly after cisplatin exposure. However, multiple pathways cause ROS production and the possibility of cytosolic sources of ROS cannot be ruled out. Future studies may utilize time-lapse live imaging of transgenic zebrafish expressing genetically encoded ROS indicators for ratiometric analysis (*e.g.* HyPer3, (Bilan et al., 2013)) after incubating with a mitochondrial oxidation dye (*e.g.* mitoSOX Red), in order to estimate mitochondrial contributions to ROS production in response to cisplatin. Using these methods, changes in ROS production may also be correlated with time-lapsed live imaging of transgenic zebrafish expressing mitoGCaMP3 in hair cells, to characterize the dynamic relationship between mitochondrial dysfunction and oxidative stress over time. Such experiments may provide further mechanistic insights to the role of mitochondria in cisplatin ototoxicity.

5. Conclusion

In summary, our results show that the function of hair cell mitochondria is acutely disrupted by cisplatin, ultimately leading to canonical caspase-3-mediated apoptosis. Specifically, cisplatin causes hyperpolarized mitochondrial membrane potential, elevated mitochondrial calcium levels, and increased ROS production. Whether these changes lead to eventual collapse of mitochondrial membrane potential and terminal mitochondrial dysfunction remain unknown, but our findings further implicate mitochondrial impairment as a critical early-stage cellular event in cisplatin ototoxicity.

Declaration of Competing Interest

None.

Author contributions

David Lee, Mark Warchol, and Lavinia Sheets designed the experiments. David Lee and Angela Schrader performed the experiments and analyzed the data. David Lee contributed to primary manuscript writing. Lavinia Sheets and Mark Warchol critically revised the manuscript. All authors approved of the final version of the manuscript.

Author statement

David Lee: Conceptualization, Methodology, Formal Analysis, Investigation, Visualization, Writing- Original draft preparation. Angela Schrader: Investigation, Formal Analysis, Visualization. Mark Warchol: Conceptualization, Methodology, Writing- Review & Editing, Supervision. Lavinia Sheets: Conceptualization, Methodology, Writing- Review & Editing, Supervision.

Statement of support

Research reported in this publication was supported by a Large-Scale Interdisciplinary Research Initiative from the Children's Discovery Institute, St. Louis Children's Hospital (LS and MW; Grant # MC-LI-2018–762) and the National Institute of Deafness and Other Communication Disorders (NIDCD) within the National Institutes of Health (NIH), through the "Development of Clinician/Researchers in Academic ENT" training grant, award number T32DC000022 (DL). The content is solely the responsibility of the authors and does not necessarily represent the official view of the funding sources.

References

Alam, S.A., Ikeda, K., Oshima, T., Suzuki, M., Kawase, T., Kikuchi, T., Takasaka, T., 2000. Cisplatin-induced apoptotic cell death in Mongolian gerbil cochlea. Hear. Res. 141 (1–2), 28–38. doi:10.1016/s0378-5955(99)00211-7.

Behra, M., Gallardo, V.E., Bradsher, J., Torrado, A., Elkahloun, A., Idol, J., Sheehy, J., Zonies, S., Xu, L., Shaw, K.M., Satou, C., Higashijima, S.-I., Weinstein, B.M., Burgess, S.M., 2012. Transcriptional signature of accessory cells in the lateral line, using the Tnk1bp1:EGFP transgenic zebrafish line. BMC Dev. Biol. 12 (1), 6. doi:10.1186/1471-213x-12-6.

Bernardi, P., 1999. Mitochondrial transport of cations: channels, exchangers, and permeability transition. Physiol. Rev. 79 (4), 1127–1155. doi:10.1152/physrev.1999.79.4.1127.

Bilan, D.S., Pase, L., Joosen, L., Gorokhovatsky, A.Y., Ermakova, Y.G., Gadella, T.W., Grabher, C., Schultz, C., Lukyanov, S., Belousov, V.V., 2013. HyPer-3: a genetically encoded H(2)O(2) probe with improved performance for ratiometric and fluorescence lifetime imaging. ACS Chem. Biol. 8 (3), 535–542. doi:10.1021/cb300625g.

Borse, V., Al Aameri, R.F.H., Sheehan, K., Sheth, S., Kaur, T., Mukherjea, D., Tupal, S., Lowy, M., Ghosh, S., Dhukhwa, A., Bhatta, P., Rybak, L.P., Ramkumar, V., 2017. Epigallocatechin-3-gallate, a prototypic chemopreventative agent for protection against cisplatin-based ototoxicity. Cell Death Dis. 8 (7), e2921. doi:10.1038/cddis.2017.314.

Brock, P.R., Knight, K.R., Freyer, D.R., Campbell, K.C., Steyger, P.S., Blakley, B.W., Rassekh, S.R., Chang, K.W., Fligor, B.J., Rajput, K., Sullivan, M., Neuwelt, E.A., 2012. Platinum-induced ototoxicity in children: a consensus review on mechanisms, predisposition, and protection, including a new International Society of Pediatric Oncology Boston ototoxicity scale. J. Clin. Oncol. 30 (19), 2408–2417. doi:10.1200/JCO.2011.39.1110.

Ciccarelli, R.B., Solomon, M.J., Varshavsky, A., Lippard, S.J., 1985. *In vivo* effects of cis- and trans-diamminedichloroplatinum(II) on SV40 chromosomes: differential repair, DNA-protein cross-linking, and inhibition of replication. Biochemistry 24 (26), 7533–7540. doi:10.1021/bi00347a005.

Devarajan, P., Savoca, M., Castaneda, M.P., Park, M.S., Esteban-Cruciani, N., Kalinec, G., Kalinec, F., 2002. Cisplatin-induced apoptosis in auditory cells: role of death receptor and mitochondrial pathways. Hear Res. 174 (1–2), 45–54. doi:10.1016/s0378-5955(02)00634-2.

Domarecka, E., Skarzynska, M., Szczepek, A.J., Hatzopoulos, S., 2020. Use of zebrafish larvae lateral line to study protection against cisplatin-induced ototoxicity: a scoping review. Int. J. Immunopathol. Pharmacol. 34. doi:10.1177/2058738420959554.

Esterberg, R., Hailey, D.W., Rubel, E.W., Raible, D.W., 2014. ER-mitochondrial calcium flow underlies vulnerability of mechanosensory hair cells to damage. J. Neurosci. 34 (29), 9703–9719. doi:10.1523/JNEUROSCI.0281-14.2014.

Esterberg, R., Linbo, T., Pickett, S.B., Wu, P., Ou, H.C., Rubel, E.W., Raible, D.W., 2016. Mitochondrial calcium uptake underlies ROS generation during aminoglycoside-induced hair cell death. J. Clin. Investig. 126 (9), 3556–3566. doi:10.1172/JCI84939.

Fernandez, K., Wafa, T., Fitzgerald, T.S., Cunningham, L.L., 2019. An optimized, clinically relevant mouse model of cisplatin-induced ototoxicity. Hear. Res. 375, 66–74. doi:10.1016/j.heares.2019.02.006.

Freyer, D.R., Brock, P.R., Chang, K.W., Dupuis, L.L., Epelman, S., Knight, K., Mills, D., Phillips, R., Potter, E., Risby, D., Simpkin, P., Sullivan, M., Cabral, S., Robinson, P.D., Sung, L., 2020. Prevention of cisplatin-induced ototoxicity in children and adolescents with cancer: a clinical practice guideline. Lancet Child Adolesc. Health 4 (2), 141–150. doi:10.1016/S2352-4642(19)30336-0.

Gentilin, E., Simoni, E., Candito, M., Cazzador, D., Astolfi, L., 2019. Cisplatin-induced ototoxicity: updates on molecular targets. Trends Mol. Med. 25 (12), 1123–1132. doi:10.1016/j.molmed.2019.08.002.

Hazlitt, R.A., Min, J., Zuo, J., 2018. Progress in the development of preventative drugs for cisplatin-induced hearing loss. J. Med. Chem. 61 (13), 5512–5524. doi:10.1021/acs.jmedchem.7b01653.

Holmgren, M., Ravicz, M.E., Hancock, K.E., Strelkova, O., Kallogjeri, D., Indzhykulian, A.A., Warchol, M.E., Sheets, L., 2021. Mechanical overstimulation causes acute injury and synapse loss followed by fast recovery in lateral-line neuromasts of larval zebrafish. Elife 10. doi:10.7554/eLife.69264.

Holmgren, M., Sheets, L., 2021. Influence of Mpv17 on hair-cell mitochondrial homeostasis, synapse integrity, and vulnerability to damage in the Zebrafish Lateral Line. Front. Cell. Neurosci. 15, 693375. doi:10.3389/fncel.2021.693375.

Kleih, M., Bopple, K., Dong, M., Gaissler, A., Heine, S., Olayioye, M.A., Aulitzky, W.E., Essmann, F., 2019. Direct impact of cisplatin on mitochondria induces ROS production that dictates cell fate of ovarian cancer cells. Cell Death. Dis. 10 (11), 851. doi:10.1038/s41419-019-2081-4.

Knight, K.R., Chen, L., Freyer, D., Aplenc, R., Bancroft, M., Bliss, B., Dang, H., Gillmeister, B., Hendershot, E., Kraemer, D.F., Lindenfeld, L., Meza, J., Neuwelt, E.A., Pollock, B.H., Sung, L., 2017. Group-wide, prospective study of ototoxicity assessment in children receiving cisplatin chemotherapy (ACCL05C1): a report from the Children's oncology group. J. Clin. Oncol. 35 (4), 440–445. doi:10.1200/JCO.2016.69.2319.

Kros, C.J., Steyger, P.S., 2019. Aminoglycoside- and cisplatin-induced ototoxicity: mechanisms and otoprotective strategies. Cold Spring Harb. Perspect. Med. 9 (11). doi:10.1101/cshperspect.a033548.

Li, M., Liu, J., Liu, D., Duan, X., Zhang, Q., Wang, D., Zheng, Q., Bai, X., Lu, Z., 2021. Naringin attenuates cisplatin- and aminoglycoside-induced hair cell injury in the zebrafish lateral line via multiple pathways. J. Cell. Mol. Med. 25 (2), 975–989. doi:10.1111/jcmm.16158.

Lu, J., Wang, W., Liu, H., Liu, H., Wu, H., 2019. Cisplatin induces calcium ion accumulation and hearing loss by causing functional alterations in calcium channels and exocytosis. Am. J. Transl. Res. 11 (11), 6877–6889. https://www.ncbi.nlm.nih.gov/pubmed/31814894.

Lu, X., Deng, T., Dong, H., Han, J., Yu, Y., Xiang, D., Nie, G., Hu, B., 2022. Novel application of eupatilin for effectively attenuating cisplatin-induced auditory hair cell death via mitochondrial apoptosis pathway. Oxidative Med. Cell. Longev. 2022 doi:10.1155/2022/1090034.

Lukasz, D., Beirl, A., Kindt, K., 2022. Chronic neurotransmission increases the susceptibility of lateral-line hair cells to ototoxic insults. bioRxiv doi:10.1101/2022.02.22.481465.

Martens-de Kemp, S.R., Dalm, S.U., Wijnolts, F.M., Brink, A., Honeywell, R.J., Peters, G.J., Braakhuis, B.J., Brakenhoff, R.H., 2013. DNA-bound platinum is the major determinant of cisplatin sensitivity in head and neck squamous carcinoma cells. PLoS ONE 8 (4), e61555. doi:10.1371/journal.pone.0061555.

Marullo, R., Werner, E., Degtyareva, N., Moore, B., Altavilla, G., Ramalingam, S.S., Doetsch, P.W., 2013. Cisplatin induces a mitochondrial-ROS response that contributes to cytotoxicity depending on mitochondrial redox status and bioenergetic functions. PLoS ONE 8 (11), e81162. doi:10.1371/journal.pone.0081162.

Ormerod, M.G., Orr, R.M., Peacock, J.H., 1994. The role of apoptosis in cell killing by cisplatin: a flow cytometric study. Br. J. Cancer 69 (1), 93–100. doi:10.1038/bjc.1994.14.

Ou, H.C., Raible, D.W., Rubel, E.W., 2007. Cisplatin-induced hair cell loss in zebrafish (Danio rerio) lateral line. Hear Res. 233 (1–2), 46–53. doi:10.1016/j.heares.2007.07.003.

Owens, K.N., Cunningham, D.E., MacDonald, G., Rubel, E.W., Raible, D.W., Pujol, R., 2007. Ultrastructural analysis of aminoglycoside-induced hair cell death in the zebrafish lateral line reveals an early mitochondrial response. J. Comp. Neurol. 502 (4), 522–543. doi:10.1002/cne.21345.

Pickett, S.B., Raible, D.W., 2019. Water waves to sound waves: using Zebrafish to explore hair cell biology. J. Assoc. Res. Otolaryngol. 20 (1), 1–19. doi:10.1007/s10162-018-00711-1.

Pickett, S.B., Thomas, E.D., Sebe, J.Y., Linbo, T., Esterberg, R., Hailey, D.W., Raible, D.W., 2018. Cumulative mitochondrial activity correlates with ototoxin susceptibility in zebrafish mechanosensory hair cells. Elife 7. doi:10.7554/eLife.38062.

Pinto, A.L., Lippard, S.J., 1985. Sequence-dependent termination of *in vitro* DNA synthesis by cis- and trans-diamminedichloroplatinum (II). Proc. Natl. Acad. Sci. U. S. A. 82 (14), 4616–4619. doi:10.1073/pnas.82.14.4616.

Prayuenyong, P., Baguley, D.M., Kros, C.J., Steyger, P.S., 2021. Preferential cochleotoxicity of cisplatin. Front. Neurosci. 15, 695268. doi:10.3389/fnins.2021.695268.

Rizzuto, R., De Stefani, D., Raffaello, A., Mammucari, C., 2012. Mitochondria as sensors and regulators of calcium signalling. Nat. Rev. Mol. Cell Biol. 13 (9), 566–578. doi:10.1038/nrm3412.

Schmitt, N.C., Page, B.R., 2018. Chemoradiation-induced hearing loss remains a major concern for head and neck cancer patients. Int. J. Audiol. 57 (sup4). doi:10.1080/14992027.2017.1353710, S49-S54.

Schneider, C.A., Rasband, W.S., Eliceiri, K.W., 2012. NIH Image to ImageJ: 25 years of image analysis. Nat. Methods 9 (7), 671–675. doi:10.1038/nmeth.2089.

Sheth, S., Mukherjea, D., Rybak, L.P., Ramkumar, V., 2017. Mechanisms of cisplatin-induced ototoxicity and otoprotection. Front. Cell Neurosci. 11, 338. doi:10.3389/fncel.2017.00338.

Theunissen, E.A., Zuur, C.L., Jozwiak, K., Lopez-Yurda, M., Hauptmann, M., Rasch, C.R., van der Baan, S., de Boer, J.P., Dreschler, W.A., Balm, A.J., 2015. Prediction of hearing loss due to cisplatin chemoradiotherapy. JAMA Otolaryngol. Head Neck Surg. 141 (9), 810–815. doi:10.1001/jamaoto.2015.1515.

Thomas, A.J., Hailey, D.W., Stawicki, T.M., Wu, P., Coffin, A.B., Rubel, E.W., Raible, D.W., Simon, J.A., Ou, H.C., 2013. Functional mechanotransduction is required for cisplatin-induced hair cell death in the zebrafish lateral line. J. Neurosci. 33 (10), 4405–4414. doi:10.1523/JNEUROSCI.3940-12.2013.

Uribe, P.M., Mueller, M.A., Gleichman, J.S., Kramer, M.D., Wang, Q., Sibrian-Vazquez, M., Strongin, R.M., Steyger, P.S., Cotanche, D.A., Matsui, J.I., 2013. Dimethyl sulfoxide (DMSO) exacerbates cisplatin-induced sensory hair cell death in zebrafish (Danio rerio). PLoS ONE 8 (2), e55359. doi:10.1371/journal.pone.0055359.

Wang, J., Ladrech, S., Pujol, R., Brabet, P., Van De Water, T.R., Puel, J.L., 2004. Caspase inhibitors, but not c-Jun NH2-terminal kinase inhibitor treatment, prevent cisplatin-induced hearing loss. Cancer Res. 64 (24), 9217–9224. doi:10.1158/0008-5472.CAN-04-1581.

Wertman, J.N., Melong, N., Stoyek, M.R., Piccolo, O., Langley, S., Orr, B., Steele, S.L., Razaghi, B., & Berman, J.N. (2020). The identification of dual protective agents against cisplatin-induced oto- and nephrotoxicity using the zebrafish model. Elife, 9. doi:10.7554/eLife.56235.

Westerfield, M., 2000. The Zebrafish Book. A Guide For the Laboratory Use of Zebrafish (Danio rerio). University of Oregon Press 4th ed..

Yang, Z., Schumaker, L.M., Egorin, M.J., Zuhowski, E.G., Guo, Z., Cullen, K.J., 2006. Cisplatin preferentially binds mitochondrial DNA and voltage-dependent anion channel protein in the mitochondrial membrane of head and neck squamous cell carcinoma: possible role in apoptosis. Clin. Cancer Res. 12 (19), 5817–5825. doi:10.1158/1078-0432.CCR-06-1037.

Yimit, A., Adebali, O., Sancar, A., Jiang, Y., 2019. Differential damage and repair of DNA-adducts induced by anti-cancer drug cisplatin across mouse organs. Nat. Commun. 10 (1), 309. doi:10.1038/s41467-019-08290-2.

Yu, D., Gu, J., Chen, Y., Kang, W., Wang, X., Wu, H., 2020. Current strategies to combat cisplatin-induced ototoxicity. Front. Pharmacol. 11, 999. doi:10.3389/fphar.2020.00999.

Zhao, H., Xu, Y., Song, X., Zhang, Q., Wang, Y., Yin, H., Bai, X., Li, J., 2022. Cisplatin induces damage of auditory cells: possible relation with dynamic variation in calcium homeostasis and responding channels. Eur. J. Pharmacol. 914, 174662. doi:10.1016/j.ejphar.2021.174662.